Application of a Constitutive Equation to Polymer Melts

RAMESH N. SHROFF and MITSUZO SHIDA, *Chemplex Company, Rolling Meadows, Illinois 60008*

Synopsis

Yamamoto's integral constitutive equation in which the memory function is dependent on the second invariant of the rate of deformation tensor at past times has been found to be successful in predicting many of the nonlinear viscoelastic functions from the linear viscoelastic data for melts of linear polyethylenes, polypropylenes, and polystryene but not for those of branched polyethylenes with high level of long-chain branching. A specific functional form for the rate-dependent relaxation spectrum is used and is based on the physical meaning resulting from the molecular entanglement theory of Graessley on steady shearing flow. No arbitrary constant is involved in such an interconversion scheme. The data examined are dynamic storage modulus and loss modulus, steady flow viscosity, first normal stress difference, and parallel superimposed small oscillations on steady shear flow. The theory predicts that in such parallel superimposed experiments, storage modulus $G'(\omega,\dot{\gamma})$ divided by the square of frequency shows a maximum under finite shear and that $G'(\omega,\dot{\gamma})$ would itself become negative at a frequency whose value is about one third the superimposed rate of shear. The experiments are in line with such predictions. Possible reasons for the failure of the theory for branched polyethylenes are considered, and a possible approach is suggested so that the interconversion scheme may be successful for such resins.

INTRODUCTION

Nonlinear rheological behavior as exemplified in the steady flow viscosity, the first normal stress difference, the time-dependent stress growth and relaxation, and the small oscillations superimposed on steady shear flow has been explained, at least semiquantitatively, through the use of various integral constitutive equations. These equations fall into two main categories. One is based on the rate of strain dependence such as in the models of Yamamoto,[1] Bird and coworkers,[2,3] Carreau,[4] Bogue,[5] and White.[6] The other category is based on the theories of strain dependence such as in the models of Bernstein, Kearsley, and Zapas,[7,8] White-Tokita,[9] and Tanner.[10] Neither category of theories with the accompanying approximations appears to be completely satisfactory in quantitatively predicting all the above-mentioned nonlinear phenomena for all polymeric materials. The purpose of this article is neither to review the various theories nor to examine the reasons for their limited application. This has been accomplished in the recent articles of Kajura et al.,[11] Yamamoto, Chen, and Bogue,[12] and Takahashi et al.[13] Rather, we have used Yamamoto's theory, in which the relaxation spectrum is dependent on the second invariant of the rate of deformation tensor, in the most general form and examined its applicability to the orthogonal superimposed data of Simmons[14] on an 8.5% polyisobutylene solution in Cetane. This is the only polymeric solution considered here.

Journal of Applied Polymer Science, Vol. 26, 1847–1863 (1981)
 CCC 0021-8995/81/061847-17$01.70

Thereafter, for reasons explained later, we introduce a specific functional form for the rate-dependent spectrum and examine its applicability to the dynamic moduli, the steady flow viscosity, and the first normal stress difference data on melts of linear and branched polyethylenes, polypropylenes, and polystyrene. The application of the theory to the parallel superimposed and transient shear stress data on linear polyethylene melts is considered only to a limited extent because of the experimental limitations discussed here.

THEORY

To explain the nonlinear viscoelastic fluid behavior, the following generalized relation represents a class of nonlinear constitutive equations[1]:

$$\sigma = \int_{-\infty}^{\infty} \mu(t - t', \|(t')) \left\{\left(1 + \frac{\epsilon}{2}\right)(C^{-1} - 1) + \left(\frac{\epsilon}{2}\right)(C - 1)\right\} dt' \tag{1}$$

where C and C^{-1} are the Cauchy and the Finger deformation tensor and its inverse, respectively; ϵ is an empirical parameter; μ is the governing memory function, which is taken to be dependent on the second invariant of the rate of deformation tensor at past times. The central problem is to determine the form of the memory functions μ that can be used to model the fluids behavior over a reasonably general set of conditions. The determination of this function has given considerable difficulties. As discussed by Yamamoto,[1] this may be due in part, to the fact that specific forms for μ have been assumed with parameters to be determined, rather than taking a completely general form.

He proposed to determine the general form of μ through the employment of an associated rate-dependent relaxation spectrum:

$$\mu(t - t', \|(t')) = \int_{-\infty}^{\infty} \frac{H(\tau, \|(t'))}{\tau} e^{-(t-t')/\tau} d \ln \tau \tag{2}$$

Using eqs. (1) and (2), and the relations for the following experimental cases were derived.

Stress growth or overshoot at the start of steady shear flow:

$$\sigma_{12}^{G}(t,\dot{\gamma}) = \dot{\gamma} \int_{-\infty}^{\infty} H(\tau) t\, e^{-t/\tau} + H(\tau,\dot{\gamma}) \{\tau - (t + \tau) e^{-t/\tau}\} d \ln \tau \tag{3}$$

$$\sigma_{n}^{G}(t,\dot{\gamma}) = \dot{\gamma}^2 \int_{-\infty}^{\infty} [H(\tau) t^2 e^{-t/\tau} + H(\tau,\dot{\gamma}) \times \{2\tau^2 - (t^2 + 2t\tau + 2\tau^2) e^{-t/\tau}\}] d \ln \tau \tag{4}$$

where $H(\tau)$ is the familiar relaxation spectrum in the linear viscoelastic theory, $H(\tau,\dot{\gamma})$ is the rate-dependent relaxation spectrum, σ_{12} is the shear stress, and $\sigma_n = \sigma_{11} - \sigma_{22}$ is the first normal stress difference. In the limit of $t \to \infty$, the steady-state values of stress are given by the relations

$$\eta(\dot{\gamma}) = \sigma_{12}(\dot{\gamma})/\dot{\gamma} = \int_{-\infty}^{\infty} H(\tau,\dot{\gamma}) \tau\, d \ln \tau \tag{5}$$

$$\psi_1(\dot{\gamma}) = \sigma_n(\dot{\gamma})/\dot{\gamma}^2 = \int_{-\infty}^{\infty} H(\tau,\dot{\gamma}) \tau^2\, d \ln \tau \tag{6}$$

Stress relaxation following cessation of steady shear flow:

$$\sigma_{12}(t,\dot{\gamma}) = \dot{\gamma} \int_{-\infty}^{\infty} \tau H(\tau,\dot{\gamma})\, e^{-t/\tau} d \ln \tau \tag{7}$$

$$\sigma_n(t,\dot{\gamma}) = 2\dot{\gamma}^2 \int_{-\infty}^{\infty} \tau^2 H(\tau,\dot{\gamma})\, e^{t/\tau} d \ln \tau \tag{8}$$

Small oscillations superimposed on steady shear flow:

$$G'_p(\omega,\dot{\gamma}) = \int_{-\infty}^{\infty} [H(\tau,\dot{\gamma}) + 8\dot{\gamma}^2 H'(\tau,\dot{\gamma})/(1+\omega^2\tau^2)] \frac{\omega^2\tau^2}{1+\omega^2\tau^2} d \ln \tau \tag{9}$$

$$G''_p(\omega,\dot{\gamma}) = \int_{-\infty}^{\infty} \left[H(\tau,\dot{\gamma}) + 4\dot{\gamma}^2 H'(\tau,\dot{\gamma}) \frac{1-\omega^2\tau^2}{1+\omega^2\tau^2}\right] \frac{\omega\tau}{1+\omega^2\tau^2} d \ln \tau \tag{10}$$

where

$$H'(\tau,\dot{\gamma}) = \frac{1}{2} \frac{\partial H(\tau,\dot{\gamma})}{\partial \dot{\gamma}^2} \tag{11}$$

Transverse of orthogonal superimposed oscillations:

$$G'(\omega,\dot{\gamma}) = \int_{-\infty}^{\infty} H(\tau,\dot{\gamma}) \frac{\omega^2\tau^2}{1+\omega^2\tau^2} d \ln \tau \tag{12}$$

$$G''(\omega,\dot{\gamma}) = \int_{-\infty}^{\infty} H(\tau,\dot{\gamma}) \frac{\omega\tau}{1+\omega^2\tau^2} d \ln \tau \tag{13}$$

where

$$G''(\omega,\dot{\gamma}) \equiv \omega\eta'(\omega,\dot{\gamma}) \tag{14}$$

EXPERIMENTAL

Materials

The polymers investigated are several samples of commercially available linear and branched polyethylenes of varying molecular weight (MW) and molecular weight distribution (MWD). The molecular parameters of these samples have appeared in previous articles.[15,16] We also consider here commercial samples of polypropylenes of varying MW and a sample of polystyrene.

Apparatus and Procedures

Information on the MW, the MWD, and, where applicable, the level of long-chain branching (LCB) is obtained using the Waters Associates gel permeation chromatograph (GPC) operated at 135°C. The solvent used in it and for intrinsic viscosity determination to obtain the LCB level is 1,2,4-trichlorobenzene. The data on the steady shear viscosity $\eta(\dot{\gamma})$, the first normal stress difference $\sigma_n(\dot{\gamma})$, the shear stress $\sigma_{12}^G(t,\dot{\gamma})$ and $\sigma_{12}(t,\dot{\gamma})$, the dynamic viscosity $\eta'_p(\omega,\dot{\gamma})$, and storage modulus $G'_p(\omega,\dot{\gamma})$ in parallel oscillations superimposed on steady shear flow are obtained in the low shear rate range using the Weissenberg Rheogoniometer (WRG) operated as a cone-and-plate instrument at 190°C. The shear rate range

is 0.001–1 sec^{-1}, but the exact range depends on the MW of the sample. Beyond 1 sec^{-1}, most samples exude out of gap. The oscillatory shear amplitude in parallel superimposed flow is 0.009 radian (0.5°). The dynamic viscosity $\eta'(\omega)$ and storage modulus $G'(\omega)$ are obtained using WRG in the radian frequency range 0.03–60 sec^{-1}. For some linear polyethylenes, independent check of $\eta(\dot{\gamma})$, $\eta'(\omega)$, $G'(\omega)$, and σ_n data is obtained from measurements in Rheometrics Mechanical Spectrometer (RMS). All sample plaques for use in WRG and RMS are stabilized with up to 0.6% Ionol (butylhydroxytoluene) to avoid chain extension and scission.

At high shear rates ($\dot{\gamma} > 3$ sec^{-1}), $\eta(\dot{\gamma})$ data on 190°C are measured using a gas extrusion rheometer with two dies having $L/D = 0$ (a sharp-edged orifice) and $L/D = 19.4$, both having entrance angle of 90°. In this rheometer, volumetric flow rates are determined at several pressures. When using the orifice, the low pressures are read on a 0–100 psi gauge with an accuracy of ± 0.1 psi. Entrance and Rabniowitsch corrections are applied as usual.

RESULTS AND DISCUSSION

Determination of $H(\tau,\dot{\gamma})$ from Stress Growth

The differentiation of eqs. (3) and (4) with respect to time shows[1] that both the shear stress and the normal stress exhibit overshoot since $H(\tau) > H(\tau,\dot{\gamma})$ and that the time of maximum of normal stress occurs after that of the shear stress. However, direct determination of $H(\tau,\dot{\gamma})$ requires either the time derivative of the difference between $\sigma_{12}(t,0)$ and $\sigma_{12}(t,\dot{\gamma})$ or the difference $\sigma_n(t,0) - \sigma_n(t,\dot{\gamma})$. In addition, the knowledge of $H(\tau)$ is required. Our own experience shows that reliable transient stress growth data are difficult to obtain because of the uncertainty in determining the onset of stress growth due to the finite response time of the instrument ($\simeq$0.02–0.08 sec). The accuracy of determining the time derivative would thus be even more uncertain. Also, for many polymers studied, here, Newtonian behavior is not quite reached at the lowest shear rate employed, and thus $\sigma_{12}(t,0)$ and $\sigma_n(t,0)$ cannot be accurately determined.

Determination of $H(\tau,\dot{\gamma})$ from Stress Relaxation

The time differentiation of eq. (7) gives

$$\frac{d\sigma_{12(t,\dot{\gamma})}}{dt} = \int_{-\infty}^{\infty} H(\tau,\dot{\gamma})\, e^{-t/\tau} d \ln \tau \tag{15}$$

Therefore, the conventional methods[17] of determining $H(\tau)$ from relaxation modulus $G(t)$ obtained in linear viscoelastic experiments can be applied in deriving $H(\tau,\dot{\gamma})$ from $d\sigma_{12}(t,\dot{\gamma})/dt$. However, as in stress growth experiments, limitations exist in determining accurately the time derivative of the stress relaxation data. For example, at long times, where the effect of shear rate is most noticeable, the stress relaxes to a fraction of the original value and sometimes does not go back to zero after waiting a long time because of a drift in electronics associated with our instrument. The time derivatives of such data would thus be even more uncertain.

Determination of $H(\tau,\dot{\gamma})$ from Superimposed Small Oscillations on Steady Shear Flow

Parallel Oscillations

Because of the appearance of $H'(\tau,\dot{\gamma})$ term in eqs. (9) and (10), it seems hopeless to try to determine $H(\tau,\dot{\gamma})$ from these type of experiments.

Orthogonal Oscillations

To those familiar with the theory of linear viscoelasticity, it is at once apparent from eqs. (12) and (13) that the conventional methods[17] of obtaining $H(\tau)$ from linear viscoelastic data, $G'(\omega)$ and $G''(\omega)$, can be applied in the direct determination of $H(\tau,\dot{\gamma})$ from $G'(\omega,\dot{\gamma})$ and $G''(\omega,\dot{\gamma})$. To our knowledge, however, the only data reported in these type of experiments are those of Simmons[14] on solutions of varying concentrations of polyisobutylene (PIB) in Cetane at 25°C. The typical data for 8.5% PIB in Cetane are shown in Figure 1. We selected $G'(\omega,\dot{\gamma})$ data for determination of $H(\tau,\dot{\gamma})$ using the computer program based on the following iterative method of Roesler and Twyman[18]:

$$H_1(\tau,\dot{\gamma}) = \left.\frac{dG'(\omega,\dot{\gamma})}{d\ln\omega}\right|_{1/\omega=\tau} \tag{16}$$

Insertion of the first approximation spectrum $H_1(\tau,\dot{\gamma})$ in eq. (12) gives $G'_1(\omega,\dot{\gamma})$. The successive approximations are then expressed by the relation

$$H_k(\tau,\dot{\gamma}) = H_{k-1}(\tau,\dot{\gamma}) + P[dG'(\omega,\dot{\gamma})/d\ln\omega - dG'_{k-1}(\omega,\dot{\gamma})/d\ln\omega]_{1/\omega=\tau}, \quad k \geq 2 \tag{17}$$

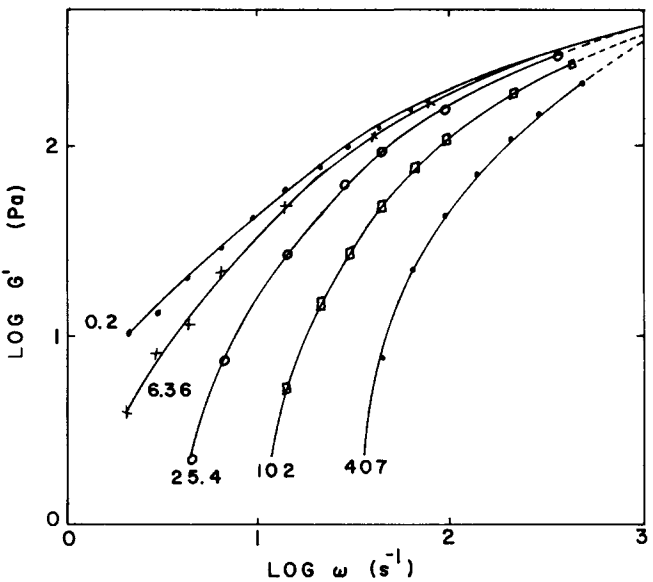

Fig. 1. Storage modulus vs. frequency for 8.54% polyisobutylene in cetane at 25°C. Typical data of Simmons in orthogonal small oscillations superimposed on steady shear flow at the shear rates indicated in the graph.

The validity of calculating the spectrum from $G'(\omega)$ is first illustrated by choosing $G'(\omega)$ data in the ω range 0.01–250 sec^{-1} for a linear polyethylene melt at 190°C and using the relations

$$G'(\omega) = \int_{-\infty}^{\infty} H(\tau) \frac{\omega^2\tau^2}{1 + \omega^2\tau^2} d \ln \tau \tag{18}$$

$$G''(\omega) = \int_{-\infty}^{\infty} H(\tau) \frac{\omega\tau}{1 + \omega^2\tau^2} d \ln \tau \equiv \omega\eta'(\omega) \tag{19}$$

From the $H(\tau)$ derived from $G'(\omega)$ using the principle of the above-mentioned iterative procedure, $G''(\omega)$ is back calculated from eq. (19) and compared with the experimental data. The agreement is good (Fig. 2), as expected, but in order to achieve a good agreement at high frequency, smooth but arbitrary extrapolation of $G'(\omega)$ data by about one decade was necessary beyond $\omega = 250$ sec^{-1}. The reason is that the data are fitted to the polynomial equation of order 3 or 4 and the extrapolation avoids sudden termination of the data at the high frequency. Without such extrapolation, the calculated values of G' are underestimated at $\omega > 40$ while with extrapolation they are slightly overestimated.

Having established the validity of obtaining the spectrum from the storage modulus, $H(\tau,\dot{\gamma})$ is similarly determined from the nonlinear $G'(\omega,\dot{\gamma})$ data for the PIB solution using eqs. (12), (16), and (17). From the $H(\tau,\dot{\gamma})$ so determined, one can test the validity of a class of constitutive equations represented by eq. (1). However, such a test could not be carried out since $\eta'(\omega,\dot{\gamma})$ data back calculated from eqs. (13) and (14) do not agree with the experimental data (Fig. 3). In particular, the original data shows the effect of the steady shearing on η' at high ω is negligible whereas it is significant on G' up to the maximum ω used in the experiments. The calculations, on the other hand, show that the effect on dynamic viscosity should also be noticeable. We feel that this inability of interconverting $\eta'(\omega,\dot{\gamma})$ and $G'(\omega,\dot{\gamma})$ for the PIB solution is reported for the first

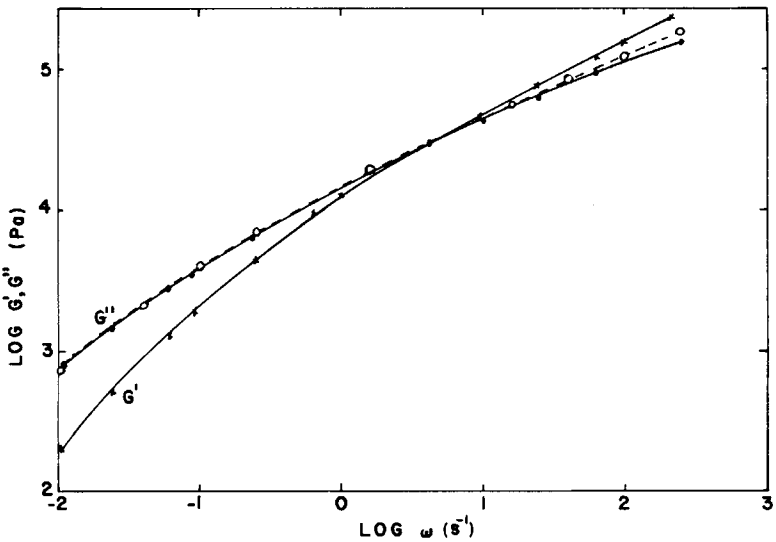

Fig. 2. Storage and loss modulus vs. frequency for a linear polyethylene melt at 190°C. Open circles are values of loss modulus calculated from relaxation spectrum derived from storage modulus.

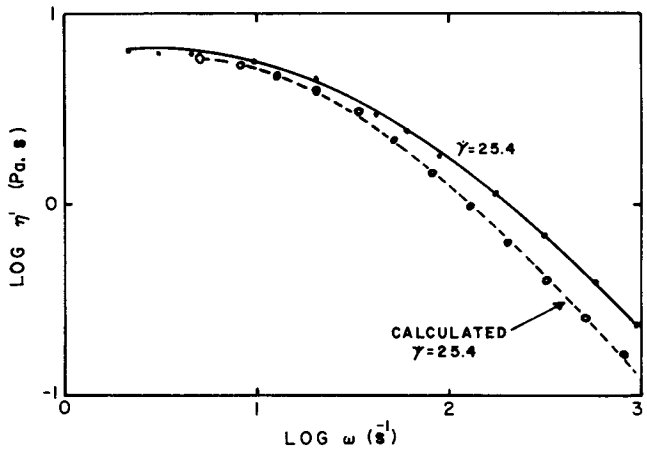

Fig. 3. Dynamic viscosity vs. frequency for 8.54% polyisobutylene in Cetane at 25°C. Data (solid points) in orthogonal small oscillations superimposed on steady shear flow at shear rate of 25.4 sec^{-1}. Open circles are calculated values from the rate dependent relaxation spectrum derived from storage modulus in the same experiments.

time and would provide yet another test for validity of a given class of constitutive equation. It is, of course, assumed that the data are reliable.

Specific Form for the Rate-Dependent Spectrum

It is now apparent that testing the validity of eq. (1) requires the orthogonal superimposed data to determine $H(\tau,\dot{\gamma})$ and then other linear and nonlinear viscoelastic data for comparison with the predicted values. Even here, the validity test for the PIB solution was unsuccessful as shown above. Van Es and Christensen[19] have provided yet another measure to test the validity of eq. (1), but the method requires transient normal stress data which depend on the instrument stiffness and cone angle in the cone-plate geometry used for making these measurements and which data are generally considered not very reliable. However, it is especially for adding the molecular significance to the rate-dependent spectrum that we introduce a specific form for the rate dependent spectrum, viz.

$$H(\tau,\dot{\gamma}) = H(\tau)\, h(\theta)\, g(\theta)^{3/2} \qquad \theta = \dot{\gamma}\tau/2 \tag{20}$$

Here, the functions $h(\theta)$ and $g(\theta)$ are the decreasing functions of θ and were introduced by Graessley[20] to explain the non-Newtonian viscosity behavior. The function $h(\theta)$ is the ratio of the rate of energy dissipation by a molecular chain divided by $\dot{\gamma}^2$ to the same quantity in the limit of $\dot{\gamma} = 0$. The function $g(\theta)$ is the ratio of the total number of entanglements between the molecules at the shear rate $\dot{\gamma}$ to the same quantity in the limit of $\dot{\gamma} = 0$. The analytic expressions for $h(\theta)$ and $g(\theta)$ as given by Graessley are

$$h(\theta) = \frac{2}{\pi}\left[\cot^{-}\theta + \frac{\theta(1-\theta^2)}{(1+\theta^2)^2}\right] \tag{21}$$

$$g(\theta) = \frac{2}{\pi}\left[\cot^{-1}\theta + \frac{\theta}{1+\theta^2}\right] \qquad \theta = \dot{\gamma}\tau/2 \tag{22}$$

As we see below, we can proceed to evaluate $H'(\tau,\dot{\gamma})$ and hence $H(\tau)$ from steady shear viscosity and then make the appropriate interconversions between various viscoelastic functions. Such an approach has been summarized earlier[15] for limited number of experiments on linear polyethylene melts, but $H(\tau,\dot{\gamma})$ was

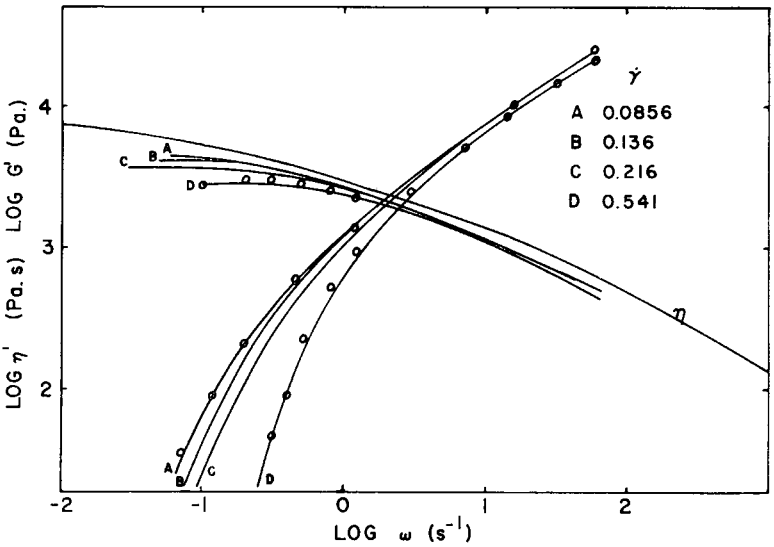

Fig. 4. Dynamic viscosity and storage modulus vs. frequency for linear polyethylene melt at 190°C. The data, represented by solid lines to avoid crowding, are from parallel small oscillations superimposed on steady shear at shear rates indicated in the graph. Open circles are calculated values from steady shear viscosity.

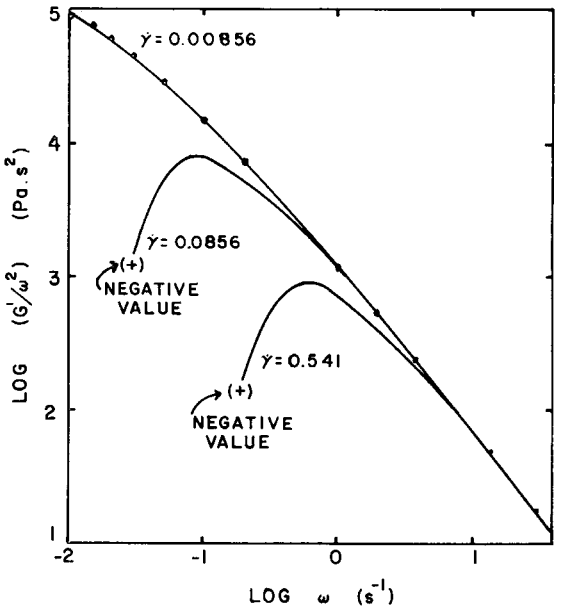

Fig. 5. Dynamic storage modulus divided by square of frequency vs. frequency for a linear polyethylene melt at 190°C. The theoretical prediction shows a maximum followed by a steep drop to negative values of the ordinate as frequency is lowered.

introduced semiempirically as a replacement for $H(\tau)$ in the linear viscoelastic theory.

We now consider the application of the specific form of the rate dependent spectrum to the data on melts of linear and branched polyethylenes, polypropylenes, and polystyrene. Parallel superimposed and stress growth data, however, are available only for linear polyethylenes.

Linear Polyethylene Melts

Use of eq. (20) in conjunction with eq. (5) allows one to determine $H(\tau)$ from $\eta(\dot{\gamma})$ using the following iterative procedure[21]:

$$H_1(\tau) = (2/\pi)\,[\dot{\gamma}\eta(\dot{\gamma})]_{1/\dot{\gamma}=\tau} \tag{23}$$

Substitution of $H_1(\tau)$ in eq. (18) and then in eq. (5) gives $\eta_1(\dot{\gamma})$. The successive approximations are expressed by the relation

$$H_k(\tau) = H_{k-1}(\tau) + P'[\dot{\gamma}\eta(\dot{\gamma}) - \dot{\gamma}\eta_{k-1}(\dot{\gamma})]_{1/\dot{\gamma}=\tau} \qquad k \geq 2 \tag{24}$$

We have thus determined both $H(\tau)$ and $H(\tau,\dot{\gamma})$, the validity of both of which is tested as follows. If they are accurate, then the calculated values of $\sigma_{12}^{G}(t,\dot{\gamma})$ from eq. (3), $\Psi_1(\dot{\gamma})$ from eq. (6), $\sigma_{12}(t,\dot{\gamma})$ from eq. (7), $G'_p(\omega,\dot{\gamma})$ from eq. (9), and $G''_p(\omega,\dot{\gamma})$ or its equivalent $\omega\eta'_p(\omega,\dot{\gamma})$ from eq. (10), $G'(\omega)$ from eq. (18), and $G''(\omega)$ from eq. (19) should agree well with the experimental data. We choose here a few examples from each experiment to illustrate the point. The agreement between the calculated and the experimental data is excellent in all cases except for branched polyethylene with high level of long-chain branching.

Despite the complexity of eqs. (9) and (10), it is encouraging to note the good agreement between both the experimental and the calculated $G'_p(\omega,\dot{\gamma})$ and $G''_p(\omega,\dot{\gamma})$ in parallel superimposed experiments (Fig. 4). Furthermore, calculations show $G'(\omega,\dot{\gamma})$ is found to be a sharply decreasing function of ω as $\dot{\gamma}$ in-

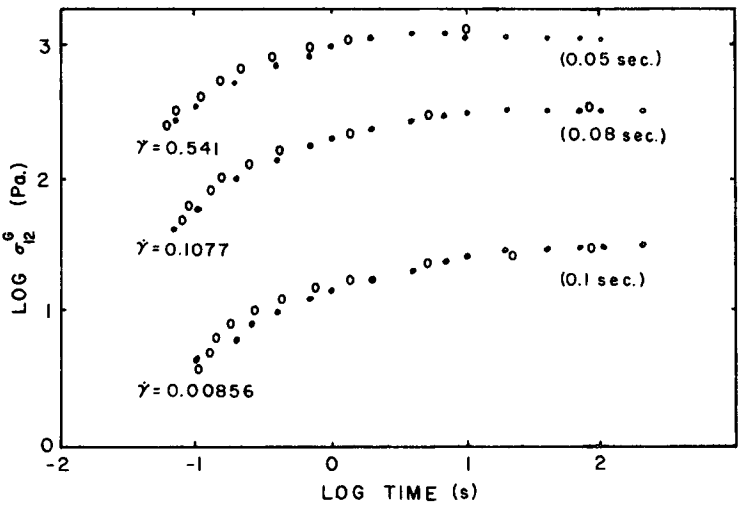

Fig. 6. Shear stress vs. time for a linear polyethylene melt at 190°C at shear rates indicated in the graph. Also shown in brackets are the instrument response times at these shear rates. Points are data, open circles are calculated values from steady shear viscosity.

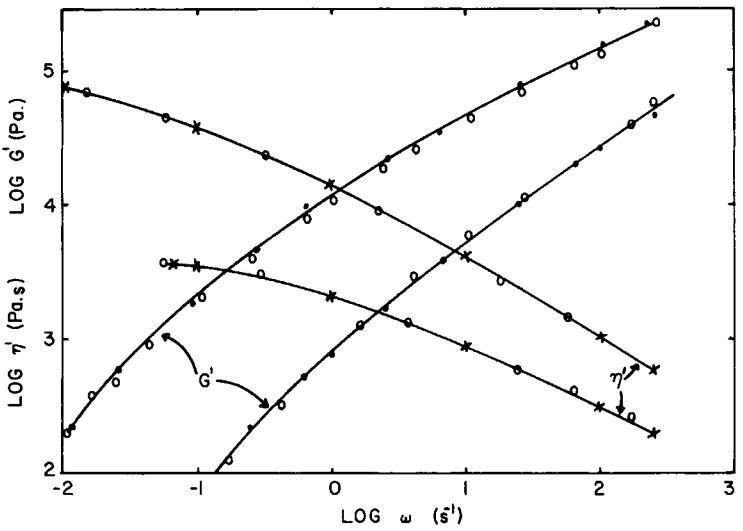

Fig. 7. Dynamic viscosity and storage modulus for two linear polyethylenes of varying molecular weight and distribution. Crosses and solid points are data, open circles are calculated values from steady shear viscosity.

creases and even becomes negative when $\omega \leqslant \dot{\gamma}/2.7$. Also the calculations show a maximum at lower frequency in a plot of $G'(\omega,\dot{\gamma})/\omega^2$ vs. ω (Fig. 5) with a maximum shifting to higher ω as $\dot{\gamma}$ increases. Experimentally, we have observed

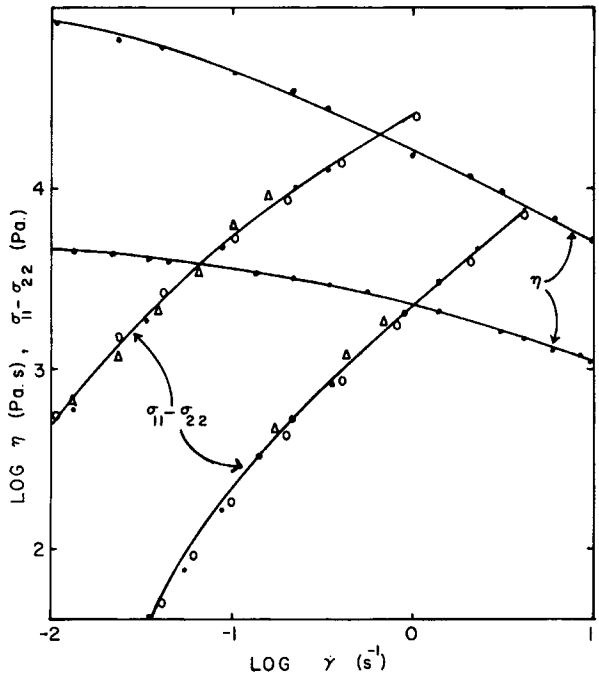

Fig. 8. Steady shear viscosity and first normal stress difference for two linear polyethylenes of varying moelcular weight and distribution. Solid points and triangles are data; open circles are calculated values from steady shear viscosity.

negative G' values at approximately the above specified ω and $\dot{\gamma}$ since the phase angle exceeded 90° by 2° or 3°. Unfortunately, we could not measure the data at even lower frequency because of experimental noise at very small amplitude. Also, at $\dot{\gamma} > 0.54$ sec^{-1}, many polymer melts exude out of the gap between the cone and the plate. The only indication of negative $G'(\omega,\dot{\gamma})$ and maximum in G'/ω^2 has been noted in experiments of Booij[22] on polymer solutions. In any case, it is encouraging that the theoretical prediction of negative $G'_p(\omega,\dot{\gamma})$ and maximum in $G'(\omega,\dot{\gamma})/\omega^2$ from the model used here is experimentally confirmed and further that $G'_p(\omega,\dot{\gamma})$ and $G''_p(\omega,\dot{\gamma})$ in parallel superimposed flows have been quantitatively predicted from the theory.

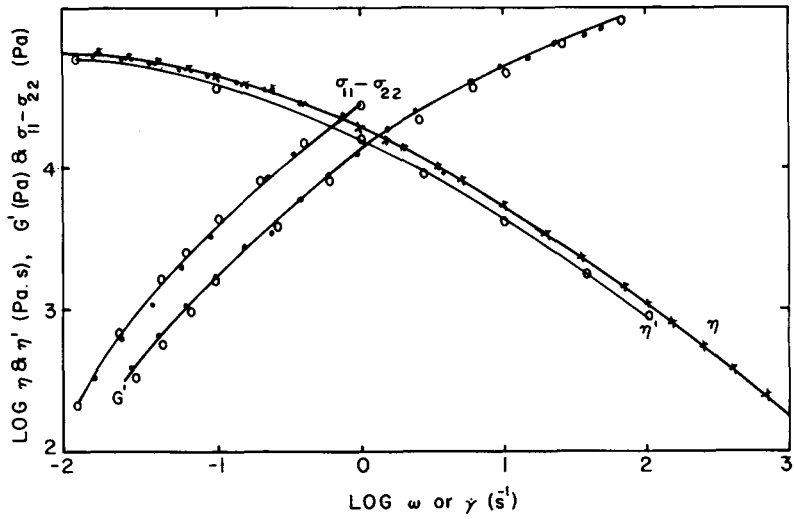

Fig. 9. Dynamic viscosity, storage modulus, steady shear viscosity, and first normal stress difference vs. frequency or shear rate for polypropylene of melt flow rate 0.8. Open circles are calculated values from steady shear viscosity. Rest of the symbols represent data at 190°C.

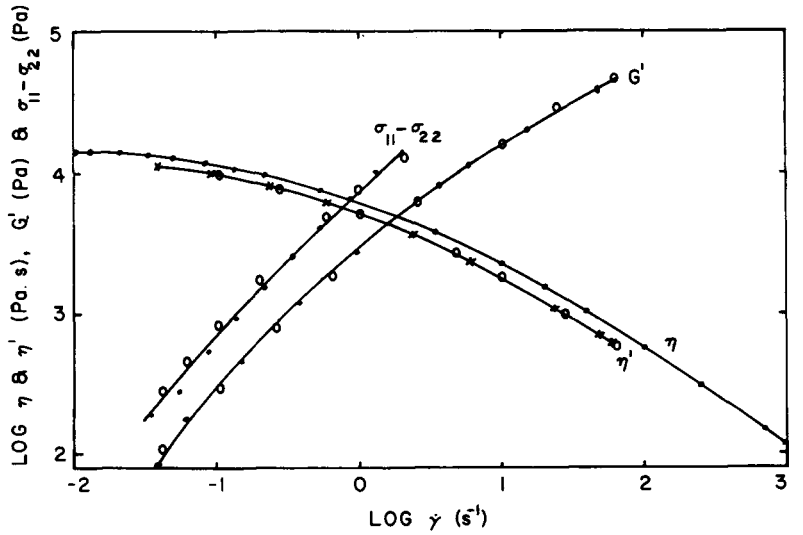

Fig. 10. Same as Fig. 9, except that data are on polypropylene with melt flow rate of 4.

The shear stress growth and relaxation data need a brief discussion. In the case of stress growth data, we found that the instrument response time for purely viscous material of the same order of viscosity is 0.05–0.1 sec^{-1} depending on the steady-state shear rate. Here, the instrument response time is defined as the time required to reach 50% of the steady-state value. This experiment on purely viscous material is done using NBS Standard Oil 27 at 0°C at which temperature

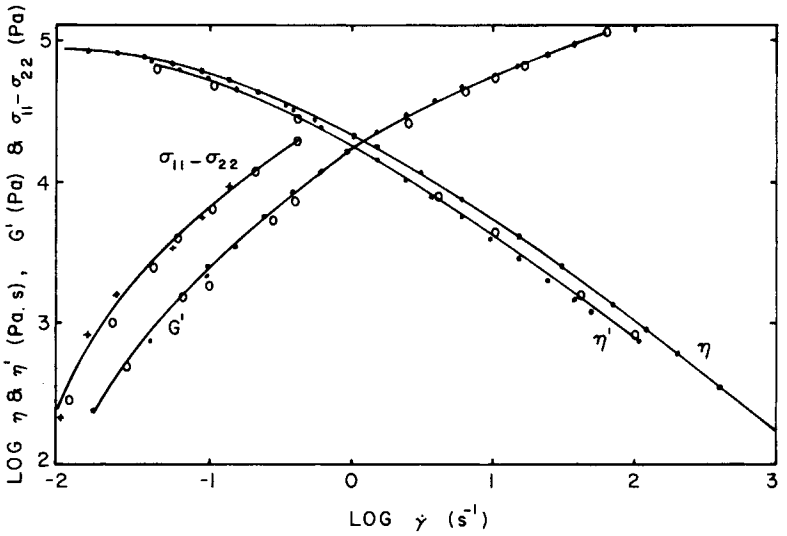

Fig. 11. Same as Fig. 9, except that data are on polystyrene.

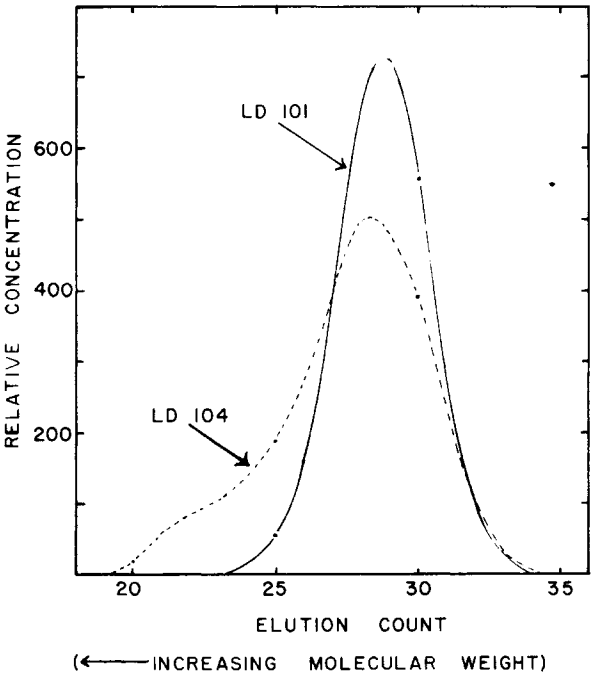

Fig. 12. Apparent molecular weight distribution for resin with high level of long-chain branching (LD 104) and with low level of LCB (LD 101).

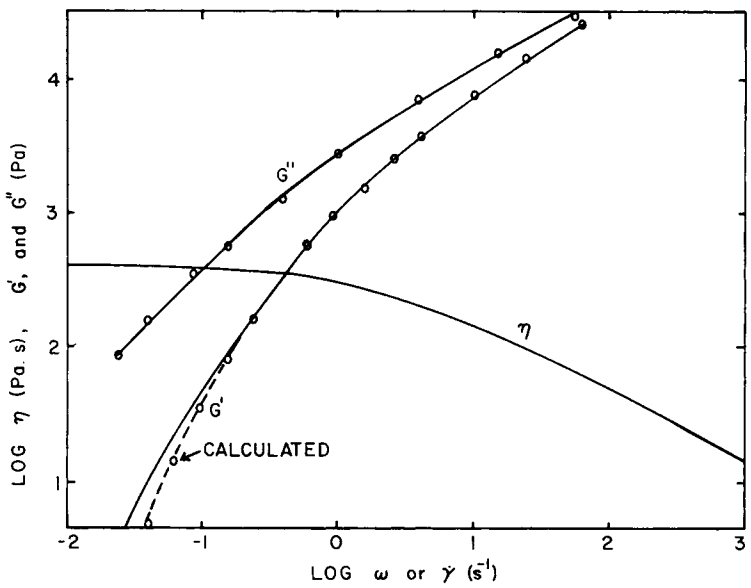

Fig. 13. Dynamic storage and loss modulus and steady shear viscosity vs. frequency or shear rate for a branched polyethylene with low level of LCB. Solid lines represent data; open circles are calculated values from steady shear viscosity.

the steady flow viscosity was 8500 poises. Accordingly, the instrument response time, defined as the midpoint of the stress growth curve obtained for this oil, was subtracted from the experimental time for the polymer melt. It is noted that this correction becomes crucial since we are plotting σ_{12}^{G} vs. t on a log–log plot instead of log–linear plot, which is commonly reported in the literature. The finite instrument response time observed for the purely viscous fluid exists despite the presence of a magnetic clutch in WRG which allows the cone rotation to be rapidly started and stopped and it needs to be determined for the stress growth and the relaxation experiment in order to determine the accurate transient data at short times.

The calculated shear stress growth data are in reasonably good agreement (Fig. 6) with the corrected experimental data. Similarly, good agreement with the stress relaxation data have been reported earlier.[15]

Precisely quantitative agreement between the values of $G'(\omega)$, $G''(\omega)$, and $\sigma_n(\dot{\gamma})$ calculated from $\eta(\dot{\gamma})$ using the principles outlined here and those measured experimentally for four linear polyethylenes of varying MW and MWD has been demonstrated earlier.[16] As an illustration, results are shown in Figures 7 and 8 for two of the resins.

Polypropylenes

The relaxation spectrum $H(\tau)$ is determined from the viscosity–shear rate data using eqs. (23) and (24). The dynamic modulus $G'(\omega)$ and dynamic viscosity $\eta'(\omega)$ are then calculated using eqs. (18) and (19). The normal stress data $\sigma_n(\dot{\gamma})$ are calculated using eqs. (20) and (6). For commercial polypropylenes of differing molecular weights and melt flow rates (melt flow rate from 0.8 to 15), agreement between the measured data and calculated values is excellent for all

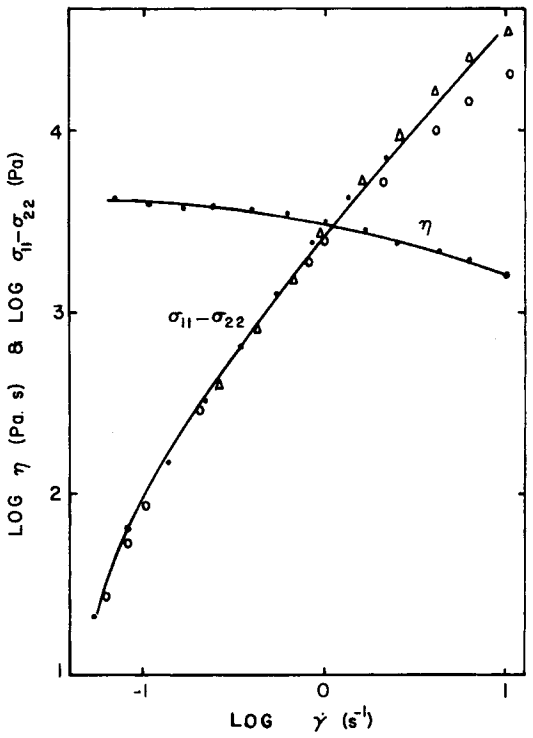

Fig. 14. First normal stress difference vs. shear rate for a branched polyethylene with low level of LCB. Open circles are calculated values from steady shear viscosity. Other symbols represent data.

the samples. The results on two resins of MFR of 0.8 and 4 are shown in Figures 9 and 10.

Polystyrene

The same procedure was applied to the data on a commercial sample of polystyrene, and here again the agreement between the calculated and the measured values is excellent (Fig. 11).

Branched Polyethylenes

Here we consider two polyethylenes—one of narrow MWD and low level of long-chain branching and another of broad MWD and high level of long-chain branching (Figure 12). In Figure 12, the raw GPC chromatograms are given. It means the high molecular weight is on the left side of the abscissa. From the GPC data and intrinsic viscosity of the whole polymer, the level of long-chain branching, as represented by n_w and g_w, is obtained using an approach outlined by Cote and Shida.[23] Here, n_w is the weight-average number of branch points per molecule, and g_w is the ratio of intrinsic viscosity of the branched polymer to that of the linear polymer of same weight-average molecular weight. The calculation of $G'(\omega)$ and $G''(\omega)$ from $\eta(\dot{\gamma})$ shows good agreement for the narrow-distribution sample (Fig. 13), but $\sigma_n(\dot{\gamma})$ data show that the calculated values

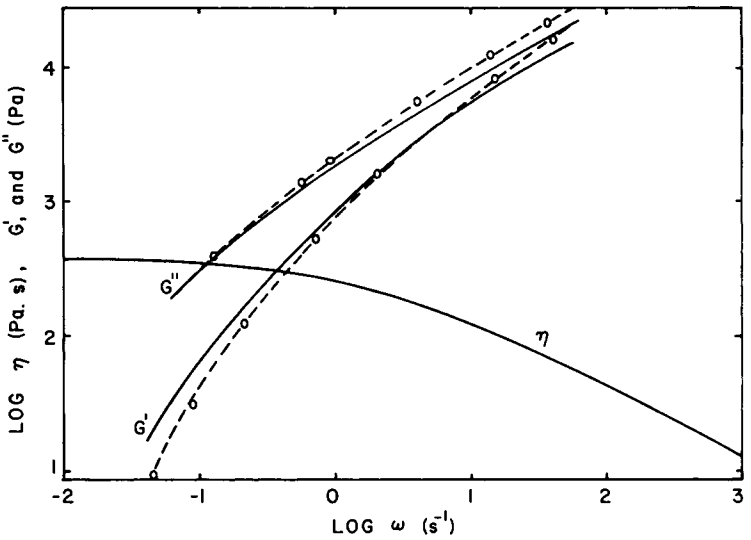

Fig. 15. Same as in Fig. 13, except that data are on a branched polyethylene with high level of LCB.

are lower than the measured data, especially at higher $\dot{\gamma}$ (Fig. 14). Such a trend is further amplified in highly branched broad MWD sample where neither of the calculated values of $G'(\omega)$, $G''(\omega)$, and $\sigma_n(\dot{\gamma})$ is in precise agreement with the measured data (Figs. 15 and 16).

It is noted that when we talk about lack of agreement between calculated and measured dynamic data, we are being precise. Many investigators may look at

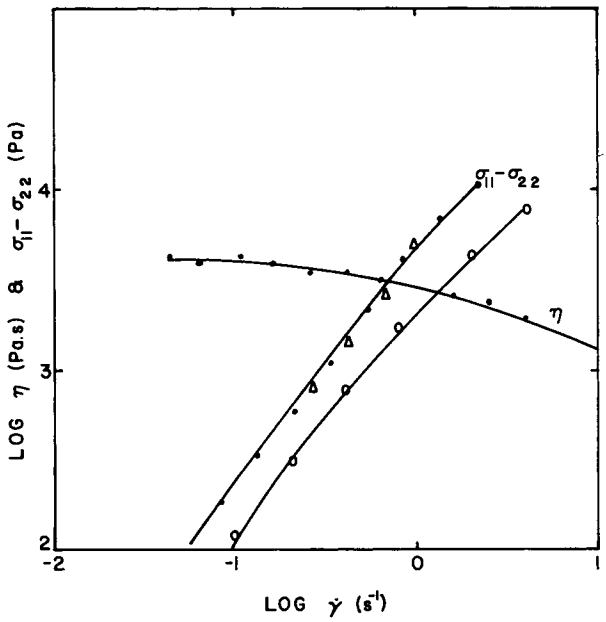

Fig. 16. Same as in Fig. 14, except that data are on a branched polyethylene with high level of LCB.

the same data in Figures 13–15 and call the agreement good. However, the discrepancy for the highly branched resin is significant (Fig. 16) when considering the normal stress data which are governed by longer relaxation times (higher molecular weight) than is the case for the dynamic data.

In order to explain the failure of quantitative interrelation between various linear and nonlinear viscoelastic quantities for the branched polyethylenes, consider the fact that both the solution and melt viscosities of broad MWD commercial, branched polyethylenes are smaller than those for the linear polymers of comparable molecular weight. The decrease in melt viscosity for branched polymers may be ascribed to a reduction in chain entanglements or other interactions between the polymer molecules in the bulk plus that due to a reduction in relaxation times. Since the relaxation spectrum on branched polymers already reflects the reduction in relaxation times, it is possible that only the modification of $h(\theta)\, g(\theta)^{1.5}$ term, eq. (20), which represents the reduction in chain entanglements, may be able to account for the observed discrepancy between the experimental and calculated values. Qualitatively speaking, a single arbitrary constant in eq. (20) which can be made to vary with the level of long-chain branching may resolve the discrepancy between the calculated and experimental data.

Conclusions

Yamamoto's integral constitutive equation in which the memory function is based on the rate-dependent relaxation spectrum has been successful in establishing quantitative relations between various linear and nonlinear viscoelastic data. A specific functional form for the rate-dependent spectrum was used based on the physical meaning that the effect of shearing is to cut off the high-molecular-weight species from contributing to a given viscoelastic response, i.e., contribution of high-molecular-weight species to any nonlinear viscoelastic function decreases as shear rate increases. In other words, polymers under shear behave as if the molecular weight distribution became narrower and narrower as shear rates keep increasing. The interconversion is successful for melts of linear polyethylenes, polypropylenes, and polystyrene but not for melts of long-chain branched polyethylenes. The experimental data considered are dynamic moduli, steady flow viscosity, first normal stress difference, and parallel small oscillations superimposed on steady shear. It is not claimed that the theory used here is universally valid, or that it is uniquely applicable to polymer melts, but that it does quantitatively account for various linear and nonlinear viscoelastic data on melts of many commerically significant polymers.

References

1. M. Yamamoto, *Trans. Soc. Rheol.*, **15**(2), 331 (1971).

2. T. W. Spriggs and R. B. Bird, *Ind. Eng. Chem. Fund.*, **4**, 182 (1964); *Chem. Eng. Soc.*, **20**, 931 (1965).

3. R. B. Bird and P. J. Carreau, *Chem. Eng. Soc.*, **23**, 427 (1968).

4. P. J. Carreau, *Trans. Soc. Rheol.*, **16**, 99 (1972).

5. D. C. Bogue, *Ind. Eng. Chem. Fund.*, **5**, 253 (1966).

6. J. L. White, *Rubber Chem. Technol.*, **42**, 257 (1969).

7. B. Bernstein, E. A. Kearsley, and L. J. Zapas, *Trans. Soc. Rheol.*, **7**, 391 (1963); *Trans. Soc. Rheol..*, **9**, 27 (1965).

8. L. J. Zapas, *J. Res. Natl. Bur. Stand. Sect.* A **70**, 525 (1966).

9. J. L. White and N. Tokita, *J. Phys. Soc. Jpn.*, **22,** 719 (1969).
10. R. J. Tanner, *AIChE J.*, **15,** 177 (1969).
11. H. Kajiura, M. Sakai, and M. Nagasawa, *Trans. Soc. Rheol.*, **20**(4), 575 (1976).
12. I. J. Chen and D. C. Bogue, *Trans. Soc. Rheol.*, **16**(I), 59 (1972).
13. M. Takahashi, T. Masuda, and S. Onogi, *Trans. Soc. Rheol.*, **21**(3), 337 (1977).
14. J. M. Simmons, *Rheol. Acta*, **7,** 184 (1968).
15. R. N. Shroff and M. Shida, *J. Polym. Sci.*, **C35,** 153 (1971).
16. R. N. Shroff and M. Shida, *Trans. Soc. Rheol.*, **21**(3), 327 (1977).
17. J. D. Ferry, *Viscoelastic Properties of Polymers*, Wiley, New York, 1977, Chaps. 3 and 4.
18. F. C. Roesler and W. A. Twyman, *Proc. Phys. Soc.*, **B68,** 971 (1955).
19. H. E. Van Es and R. M. Christensen, *Trans. Soc. Rheol.*, **17**(2), 325 (1973).
20. W. W. Graessley, *J. Chem. Phys.*, **47,** 1942 (1967).
21. R. N. Shroff, *J. Appl. Phys.*, **41,** 3652 (1970).
22. H. C. Booij, *Rheol. Acta*, **5,** 215 (1966).
23. J. A. Cote and M. Shida, *J. Polym. Sci. Part A-2*, **9,** 421 (1971).

Received June 24, 1980
Accepted October 14, 1980